Procedia Manufacturing

Volume 5, 2016, Pages 684–695

44th Proceedings of the North American Manufacturing Research Institution of SME http://www.sme.org/namrc

Pulsed Laser Assisted Micro-Scribing of Metal Thin Films in Air and Underwater using UV, Visible and Near-IR Wavelengths

Srinagalakshmi Nammi[1, a*], Nilesh J Vasa[1, b], Balaganesan G[1, c] and Anil C Mathur[2, d]

[1]*Indian Institute of Technology, Madras, India.*

[2] *Indian Space Research Organization, Ahmedabad, India.*

[a]*snl.nammi@gmail.com,* [b] *njvasa@iitm.ac.in,* [c]*gbganesh@iitm.ac.in,* [d]*acmathur@sac.isro.gov.in*

Abstract

A comparative study has been made for micro-scribing of copper and aluminum thin films in air and underwater using 355 nm, 532 nm and 1064 nm wavelengths of a Q-switched Nd^{3+}: YAG laser with 6 ns pulse duration. For aluminum in air medium, the channel depth obtained is high for 355 nm wavelength, whereas for copper coated on a polyimide substrate, 532 nm wavelengths produced higher depth. In underwater scribing, with increase in the pulsed laser energy, the depth of micro channel was increased and remained unchanged at higher energy. The influence of beam profile on the micro channel cross-section has also been discussed. Further, theoretical modeling of the laser-material interaction in air and underwater ambience conditions to estimate the recession rate has been discussed by incorporating the laser ablation temperature measured using the laser induced breakdown spectroscopy technique.

Keywords: Laser micro scribing, Ambience, Copper, Micro machining, Parabolic reflector

1 Introduction

In communications satellites thin sheets of aluminum/copper coated with polyimide substrate are used in parabolic antennas. The reflector surface has periodically spaced conductive grids with size ranging in the order of micrometer. These conductive grids operate as polarization sensitive and frequency selective surfaces. The size and shape of the grids affect the reflector function. The conductive grids on a polyimide plastic substrate are fabricated by mechanical methods that involve cutting of thin metal sheets into precise strips and pasting them in parallel lines on the surface of the reflector. Research is widely carried out in line with accurate and reliable manufacturing processes of

 Selection and peer-review under responsibility of the Scientific Programme Committee of NAMRI/SME

doi:10.1016/j.promfg.2016.08.056

these conductive grids. The pulsed laser ablation (PLA) technique has been widely studied as an effective method for the ablation of thin metal films. Laser processing of metal coated surfaces offers a number of advantages over the conventional techniques (Jackson, 2003). These include, limited heat affected zone due to nanosecond order laser pulse width, non-contact process and processing in different ambient conditions is possible. A nano second pulsed Nd^{3+}: YAG laser with a Gaussian beam profile has been used for micro-manufacturing applications, such as drilling, cutting and so on (Fabbro, 1990). Removal of material occurs due to the interaction of the intense electromagnetic waves in the laser radiation with the work piece, leading to heating, melting and vaporization of a selective micro volume. In contrast with a conventional machine tool process, laser machining does not experience tool wear, vibrations and burr formation; material removal depends on the optical and thermal properties of the workpiece (Aurich, 2009).

Nano second laser pulse is absorbed by the workpiece and through heat conduction vaporizes a focused volume of material. The ejected vapour interacts with the incoming laser beam and forms a plasma plume. Depending on the ambient conditions, the plasma plume exerts a recoil pressure, expelling the melt pool that gets redeposited at the edge of the crater or channel (Chien, 2009). In order to avoid this redeposition of expelled material on the workpiece surface, many techniques are being used that includes high pressure gas/liquid. Increase in depth with significant decrease in thermal damage was observed when machining silicon underwater. Also the debris formed due to machining was found to be carried away by water preventing redeposition (Choo, 2004). Different methods to provide water in the working zone for underwater laser etching of silicon have been reviewed and it was observed that the etch rate increase in the case of water as compared to that of air (Kruusing, 2004). Underwater laser ablation of aluminum is shown as a cost effective drilling process compared to dry ablation, with improvement in the crater shape quality (Krstulović, 2013). Metal plates of varying thicknesses have been drilled using an Nd^{3+}: YAG laser in water and air and the material removal in underwater drilling is 10 times more than in air due to the plasma confinement by water. Bubble formation and collapse due to vapourization of water is shown to be an effective method for removal of debris in wet ablation process. (Lu, 2004)

Four different lasers were studied for scribing of thin-film photovoltaic materials CdTe, CIS, SnO, ZnO, and MO (Compaan, 1996). Excellent scribe profiles were observed with the excimer laser on MO and ZnO. It is stated that optimum energy density for most efficient removal of material during scribing is strongly dependent on the wavelength of the laser used (Compaan, 1996). While scribing multilayered copper indium gallium selenide (CIGS) solar cells deposited on polyamide substrate choosing an appropriate laser wavelength is the key to keep the energy coupled in a well-defined volume at the interlayer interface. Further an overlap of laser pulses must be cautiously controlled to evade micro cracking and peeling of the top-contact layers induced by the laser pulses. Using multiple scans smooth scribe was achieved with 10 times reduced laser power (Stafe, 2012).

Most of research groups have reported on the underwater laser ablation process by using infrared wavelengths. However, there is a need to understand the behavior of laser ablation of Al/Cu films for a wide range of laser wavelengths. Laser scribing of reflective materials, such as Cu and Al films has not been studied in detail. Micro machining on thin copper films was performed for three laser wavelengths (355 nm, 532 nm and 1064 nm) and the effect of intensity and processing rate on the surface morphology has been investigated in air (Tunna, 2001). Free-electron thermal conductivity is high in these metals and it makes the controlled machining of reflective materials using laser a challenging task. However, there are very few reports on the same using the ns-pulsed Nd^{3+}:YAG laser in particular. This paper aims at presenting certain results related to underwater laser scribing using UV (355 nm), visible (532 nm) and IR (1064 nm) wavelengths of a Q-switched Nd^{3+}:YAG. The influence of various laser parameters such as laser beam profile, wavelength and ambient condition has been studied to develop laser scribing techniques for manufacturing micro-channels on Al/Cu film deposited on a flexible substrate. Further, the laser induced breakdown spectroscopy (LIBS) technique has been proposed and demonstrated for estimating the plume temperature during the laser scribing of

thin films. The estimated plume temperature has been incorporated in the theoretical modeling to understand the effect of different wavelengths (355 nm, 532 nm and 1064 nm) on a thin copper sample and the results are discussed.

2 Experimental Setup

Figure 1 shows the schematic diagram of experimental setup. A Q-switched Nd^{3+}: YAG laser with a primary wavelength of 1064 nm, a pulse width of 6 ns (Full width at half maximum, FWHM) and a repetition rate of 10 Hz was used in the present study. The laser beam was directed on to the workpiece using beam alignment optics, such as dichoric mirrors and a quartz lens with a focal length of 100 mm. Beam shaping optics (pi-Shaper, Adl Optica optical systems) was integrated for converting the Gaussian laser beam profile into a flat-top laser beam profile. By means of refractive field mapping system, the input Gaussian beam is converted into a collimated flat-top beam. The flat-top laser beam was focused using conventional optics and the laser scribing was performed near the image plane. The flat-top laser profile distribution has a large operational distance which enables the beam to be effortlessly resized using conventional optics. Laser scribing was performed on 150 µm thickness Al film and 35 µm thickness Cu films on a 50 µm thick polyimide substrate. Experiments in air medium were performed by mounting the workpiece on a motorized X-Y stage. On the other hand, experiments in underwater medium with de-ionized water were performed by fixing the workpiece in a water beaker placed over the X-Y stage. During laser induced breakdown spectroscopy (LIBS) study, the optical emission was collected at an angle of 30° by a lens of focal length 150 mm and was focused onto an optical fiber (core diameter 600 µm, NA 0.39). A spectrometer (UV-VIS2000, Ocean Optics) coupled with the fiber was used for the detection of spectral information. Surface characterization after the scribing process was carried out using a non-contact optical profilometer (Contour GT-I, Bruker and MarSurf WM100, Marh). Depth and width of the micro channels produced by scribing process were measured using a non-contact profilometer.

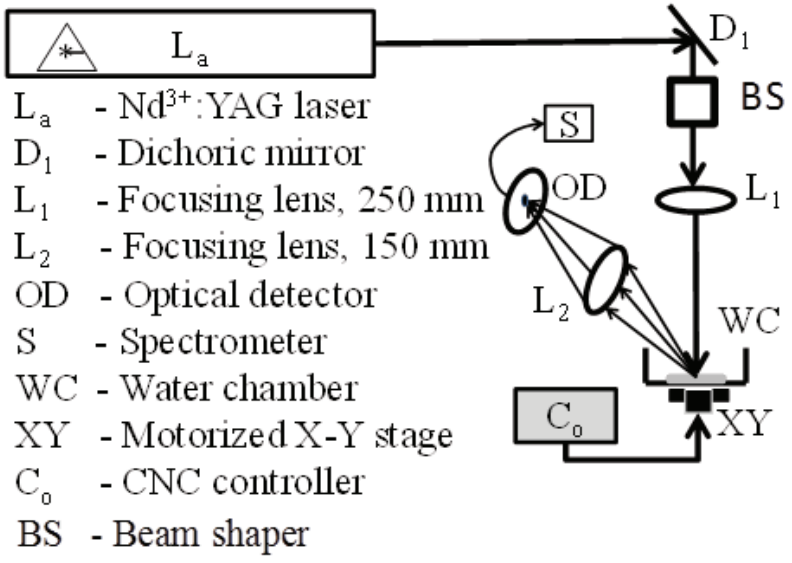

Figure 1: Schematic of the experimental setup used to produce micro channels

Table 1: Parameters and specifications used in the experiment to study the influence of wavelength and ambience

Parameters	**Specifications**
Laser used	Nd^{3+}:YAG (λ=355, 532 and 1064 nm)
Pulse duration (Frequency)	5 ns (5 Hz)
Cu and Al sample size	20 mm x 20 mm
Focal length	250 mm
Spot size (estimated)	≈ 200 μm
Beam overlap	95%
Ambient condition	Air, water (1 -10 mm above the sample)

2.1 Scribing of copper thin film coated on a polyimide substrate

The variation in depth of the scribed micro-channels on Cu films, against different laser energy maintained for ablation with three different wavelengths of 355 nm, 532 nm and 1064 nm in air is shown in Figure 2(a). For 95% overlap of the laser spot diameter and 45 mJ of energy, 532 nm wavelength laser achieved a depth of ~21 um compared to ~12 um using 355 nm and ~5 um using 1064 nm. For the energy less than 25 mJ, depths attained with 355 nm and 532 nm were similar. As the laser energy was increased, the depth reduced for 355 nm wavelength compared to 532 nm. Further, as shown in Figure 2(b), the channel depth achieved was less compared to air for both 532 and 355 nm wavelengths. However, for 1064 nm Cu showed an opposite trend; the micro channel depth for underwater scribing was ~ 7um compared to ~4 um produced in air as seen in Figure 2(b). Typical re-deposition around the edges with the laser wavelength of 532 nm for the micro channels produced in air is shown in Figure 3(a). On the other hand, underwater scribing of Cu thin films resulted in a reduction in the re-deposition of the ablated material as seen in Figure 3(b). The change in width of the channel with respect to increase in laser energy was observed to be in few tens of microns.

2.2 Scribing of aluminum thin film

The ablation depth in air is seen to be increasing with increasing energy as seen in Figure 4(a), but laser ablation depths achieved in water medium tends to increase and start to reduce/ saturate after ~5 mJ energy as shown in Figure 4(b). It was observed that the ablation depth of micro channels produced in Al through underwater laser scribing was 6 times greater compared to the depth achieved in air for all the 3 wavelengths i.e. 355 nm, 532 nm and 1064 nm, respectively. Figures 4(b) show the variation in depth of the scribed micro-channels on Al films, against different laser energies ablated with three different wavelengths of 355 nm, 532 nm and 1064 nm in air and water mediums. It was observed that a depth of ~ 100 um was achieved using both 355 nm and 532 nm with 4 mJ of energy and using 1064 nm, 80 um depth was achieved while maintaining the same laser energy. The depth achieved for ablation in air medium, using 1064 nm wavelength with 4 mJ of energy is 10 um which is less compared to the 20 um depth achieved using 355 nm and 532 nm respectively. The width of the micro

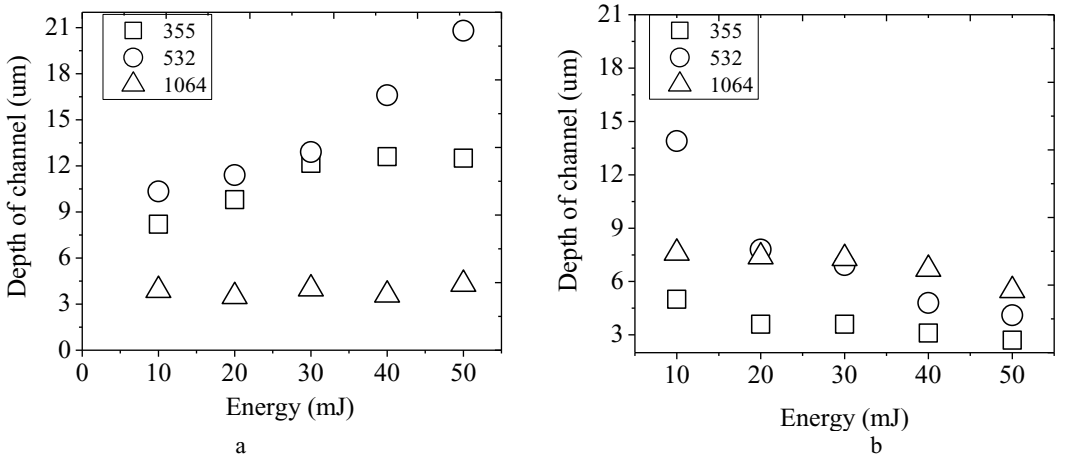

Figure 2: Depth variation of micro channels produced on copper coated polyimide thin films for three different wavelengths in a) air and b) water

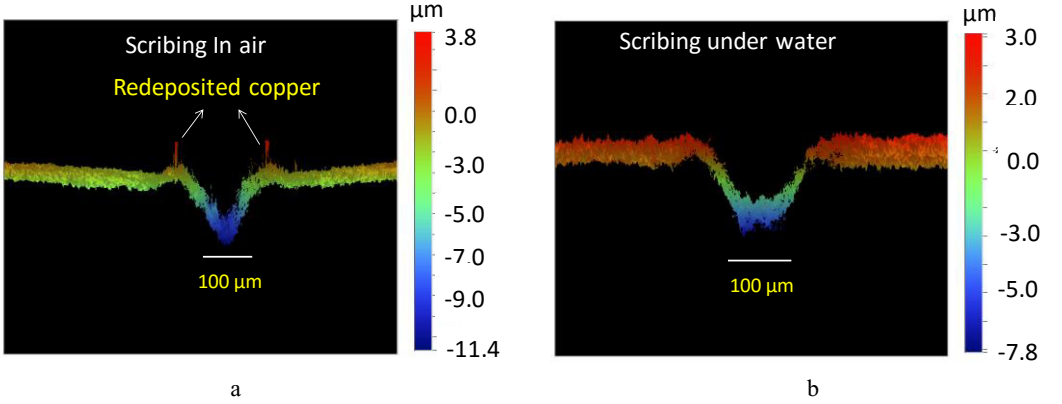

Figure 3: 3D non contact profilometer images for micro channels produced on copper thin film using 20 mJ energy for 532 nm laser wavelength in a) air and b) underwater ambience conditions

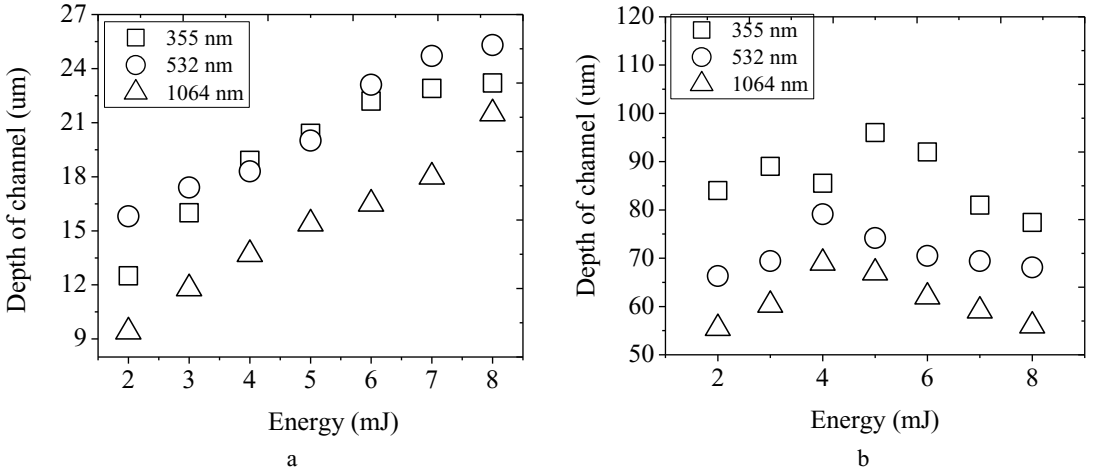

Figure 4: Depth variation of micro channels produced on aluminum coated polyimide thin films for three different wavelengths in a) air and b) water

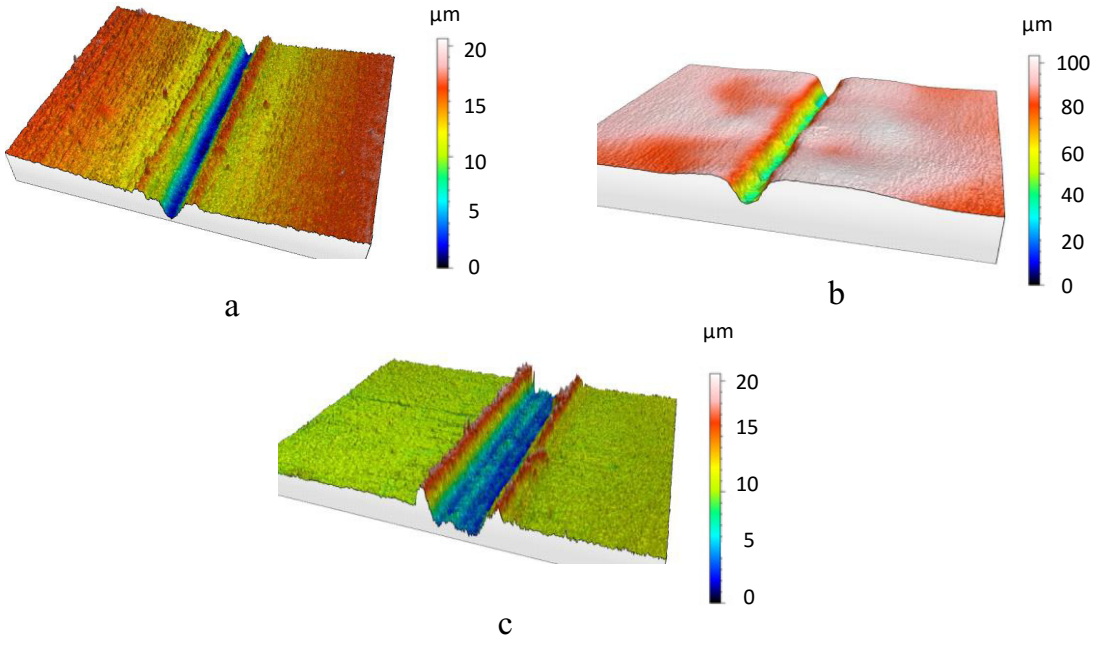

Figure 5: 3D images of the micro channels produced using 532 nm laser wavelength using a) 35 mJ energy using a Gaussian beam on copper thin film b) 7 mJ of energy using a Gaussian beam on a aluminum thin film c) 35 mJ of energy using a flat-top profile on a copper thin film. Measurements were performed using Marsurf CWM 100.

channels obtained for energies up to 4 mJ was ~ 160 um and was found to increase to ~200 um for 7 mJ and remained unchanged with further increase of energy. This shows a slight increase in the depth of the channel with increase in energy but then after threshold energy the change in width is negligible for both air and water. Preliminary studies were performed by varying the water level from 2 mm to 10 mm. At 2 mm level, spilling water on the lens during the laser ablation was observed. On the other hand, as the height of water channel was increased, the depth of the micro channel was reduced due to the plasma quenching. Hence, the water level above the workpiece was maintained at a level of 3 mm for both copper and aluminum work pieces during underwater micro scribing. Figures 5(a) and 5(b) show typical 3D optical profilometer images of micro channels produced using 532 nm laser wavelength on copper and aluminum thin films, respectively. Underwater micro channels show a wavy and distorted structure compared to the micro channel produced in air due to the disturbance caused by vapor bubbles while scribing

2.3 Influence of laser beam profile

The influence of laser beam profile on the formation of micro channel was studied for laser wavelength of 355 and 532 nm. Rectangular grooves were produced using flat-top laser profile with an overlap of 95% of the laser spot diameter. A typical 3D optical profilometer image of a micro channel produced in air is shown in Figure 5(c) for 35 mJ of energy using the wavelength of 532 nm. The depth achieved and the recast layer formation around the edges were similar to that achieved using the Gaussian laser beam profile.

3 Discussion

It was observed that for both the metals, namely Cu and Al, with increase in energy, ablation depth was increased but at higher energy levels the increase in the channel depth was reduced and almost remained unchanged. In a study conducted (Lee,2001), it was found that the shorter wavelength (in the UV region) caused a large absorption of laser energy on the surface and led to a higher temperature rise at the interface leading to a lower threshold fluence value. This is supported by the fact that the surface reflectivity for Cu is 0.45 for 355 nm, 0.62 for 532 nm and 0.97 for 1064 nm, and the absorption coefficient is 7.1×10^5 cm^{-1} for 355 nm, 6.1×10^5 cm^{-1} for 532 nm, and 8.1×10^5 cm^{-1} for 1064 nm (Palik, 1997). Since the absorption depth is high for 532 nm, it was possible to achieve a greater depth in comparison with 355 nm and 1064 nm for the same energy. Moreover, at high energies the micro channels produced using 355 nm wavelength showed a higher heat affected zone around the channel edges, which is an indication of plasma formation and subsequent heating of the workpiece.

The formation of plasma above the processing surface can lead to shielding of the work piece surface from the incident beam, thereby preventing the incident beam from coupling to the work piece surface. Previous experimental investigations into the interaction of a short wavelength laser with various metals and ceramics have shown that the formation of plasma above the work piece surface can lead to decoupling of the incident beam from the work piece surface In underwater scribing, as the water level above the work piece decreases, ablation rate increases resulting in increased depth of the scribed channel. No re-deposition at the edges is observed when micro scribing is done in DI water medium. If the work piece is covered with a water layer, the plasma is confined and its expansion is delayed. Therefore, the induced pressure is 4 to 10 times greater than the corresponding one obtained in air medium and the shock wave duration is 2–3 times longer than in the air regime at the same power density (Peyre, 1995). This results in higher material removal rates resulting in high ablation depth. Copper has less reflectivity at shorter wavelengths; reflectivity also plays a role in underwater laser scribing. The sudden increase in temperature due to the laser pulse induces shock waves caused by the cavitation bubbles that expand and collapse forming a high pressure liquid jet. These shock waves are reflected by the work piece and are reflected back from the air-water interface and increase the impact on the work piece. Because of high reflectivity of Al, depth in water is higher for all wavelengths, whereas Cu has lesser reflectivity at shorter wavelength which explains the reduced depth. The micro channel depth is increasing for Al with energy but after certain value of laser energy (5 mJ-6 mJ) depth decreases. It is because of the parasitic plasma occurring in confining water. It has been (Peyre, 1995) reported that above a 10 GW/cm^2 laser intensity threshold, a saturation of the peak pressure is shown to occur while the shock wave duration is reduced by parasitic plasma occurring in the confining water. This phenomenon occurs at the surface of the water rather than within the water volume which leads to absorption of the incident laser energy, and the laser fluence reaching the target gradually decreases.

It was observed experimentally using 20 J/cm^2 fluence for 3, 4 and 5 pulses, the depth achieved is 3.6, 4.3 and 5.2 μm, respectively. From this data, it is inferred that for one pulse the depth is ~ 1 μm. The depth achieved for 532 nm from the present model at 3000 K is thus validated with the experimental data. Figure 7 shows the temperature profile estimated using for the 3 wavelengths for Cu sample. In the developed model, as we have not incorporated the effect of plasma and the change in material properties with temperature, both 355 nm and 532 nm laser follow the same trend, but since the reflectivity of 1064 nm for same fluence is high the temperature reached at the surface is less than 355 nm and 532 nm. Same is the case with recession rate estimated and shown in Figure 8. This is also proved experimentally that 1064 nm gives lesser depth compared to shorter wavelengths. This model can further be developed by incorporating the effect of temperature on the material properties of the work piece in order to correctly predict the laser material interaction.

4 Theory of laser ablation of thin films

The temperature distribution inside the target is calculated by means of the heat conduction equation and the algorithm for calculating the temperature and recession rate is shown in section 3.1. Initially the copper target is at room temperature; as a result of the laser irradiance the target is heated. In the current model, it is assumed that the absorption coefficient and the thermal conductivity of the target layer drop to zero as soon as the temperature of that particular layer reaches 9000 K. This condition is applied in order to indicate that the material has been removed and the remaining laser energy will reach the next layer. The plasma electron temperature was calculated as 9000 K which is assumed as the temperature at which ablation takes place. The plasma electron temperature is estimated based on Boltzmann - Saha method (Descoeudres, 2004) using the emission spectrum capture using laser induced breakdown spectroscopy.

Table 2 Parameters and specifications used in to modeling the influence of wavelength on Cu thin films

Parameters	**Specifications**
Wavelength	355 nm, 532 nm, 1064 nm
Pulse duration	5 ns
Pulse Fluence	20 J/cm^2
Cu sample size	60 µm x 10 µm
Spot size (estimated)	50µm
Reflectivity	0.45 (355), 0.65 (532), 0.97 (1064)
Absorption Coefficient	7.1×10^5 cm^{-1}(355), 5.8×10^5 cm^{-1}(532), 8.6×10^5 cm^{-1}(1064)
Copper vapourization temperature	2836 K

4.1 Flow chart for measuring temperature

In metals, light is absorbed by interaction with electrons. As the pulse width of laser is of the order of few ns, which is quite longer than that of the energy relaxation time (of the order of 10^{-13} s for metals) (Bogaerts, 2003), collision with lattice phonons results in transfer of the absorbed energy to the lattice. A thermal model of the laser irradiation on a solid Cu / Al films is developed and studied to understand the phenomenological changes happening during the laser ablation process. The temperature distribution inside the target is calculated by means of the heat conduction equation as shown in flow chart in Figure 6. Laser irradiance I(x, t), a function of position and time, is the source of energy used for ablating the target. According to Beer-Lamberts law (Bogaerts, 2003)

$$I(x,t) = I_o(t)\exp(-\alpha x)\left[1-\check{R}\right] \quad (1)$$

where Ř is reflectivity and I_o (t) is the laser fluence at time t. When a pulse of laser energy is incident on the target surface, it interacts with the material and the lattice temperature increases accordingly.

When the temperature reaches the melting point of the target material, phase change is initiated and the temperature remains almost constant. After the solid to liquid phase transformation, the temperature again tends to increase and as it reaches the boiling point, the material starts to vaporize. The vapor pressure is given by Clausius-Clapeyron equation

.

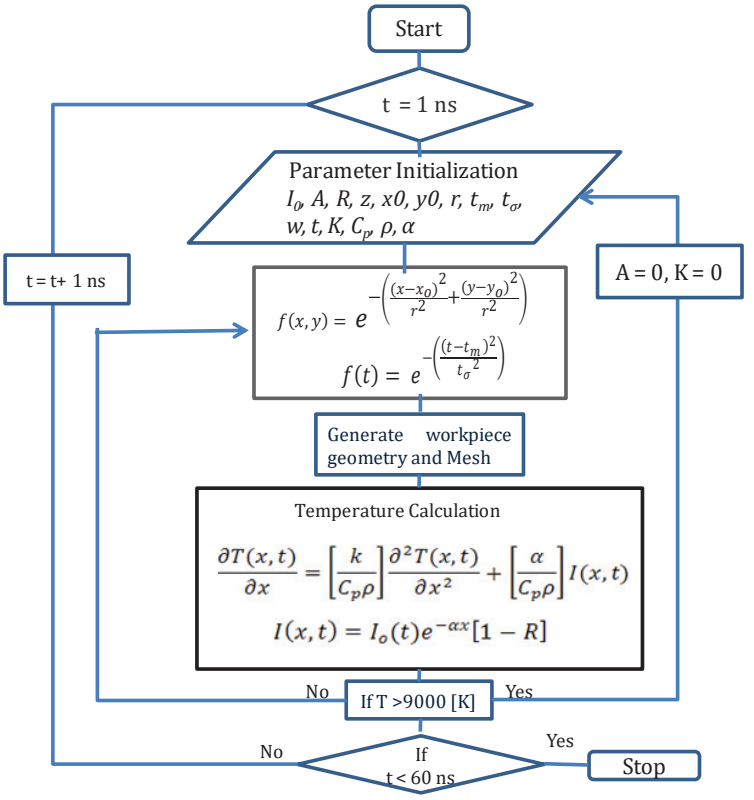

Figure 6: Algorithm used to estimate the temperature at particular position and time inside the sample

$$p_{vap}(T_s) = p_o exp\left[\frac{\Delta H_{lv}(T_s - T_b)}{RT_sT_b}\right] \quad (2)$$

where T_s and T_b are the surface temperature and the normal boiling point respectively, pressure p_0 is 1 atm, ΔH_{lv} is the latent heat of vaporization, and R is the gas constant. The flux of evaporated atoms is obtained from the vapor pressure at the surface temperature by the following equation (Bogaerts, 2003),

$$j_{evap}(T_s) = \frac{A_p(T_s)}{\sqrt{2\pi MRT_s}} \quad (3)$$

where M is the molecular mass of the atoms (kg) and ρ the mass density (kg/m^3). The surface recession rate due to evaporation is calculated from the flux of evaporated atoms using equation

$$R_{recession} = \frac{dx_{evap}}{dt} = \frac{j_{evap}\, M}{\rho} \quad (4)$$

4.2 Theoretical modeling Results for Cu thin film

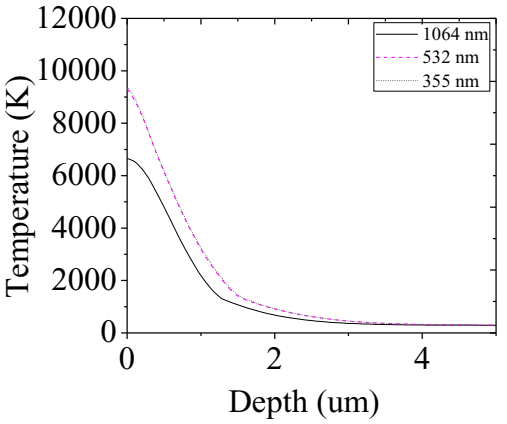

Figure 7: Temperature plot for Cu along the depth profile for 3 different wavelengths

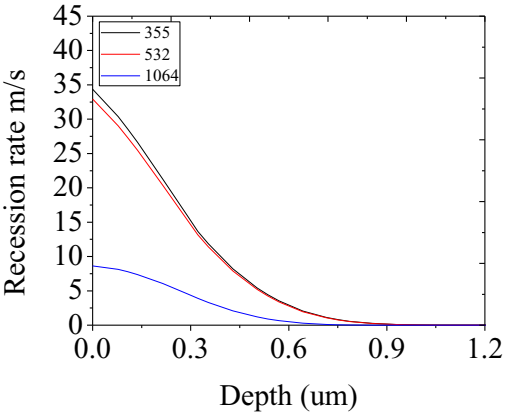

Figure 8: Recession rate for Cu along the depth profile for 3 different wavelengths

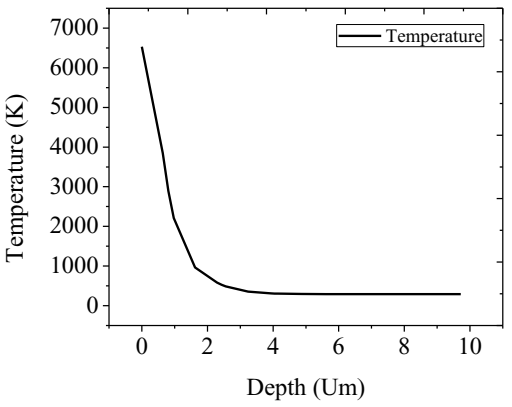

a

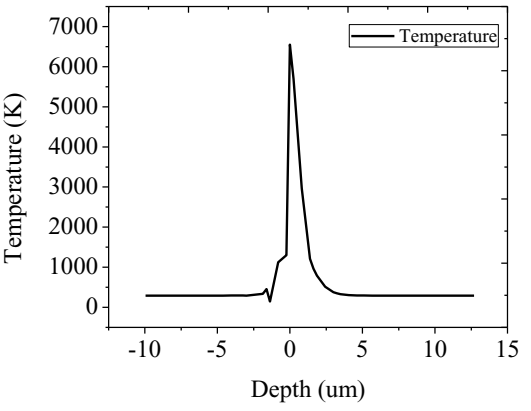

b

Figure 9: Temperature profile obtained for 532 nm laser wavelength after 12 ns a) in air b) underwater

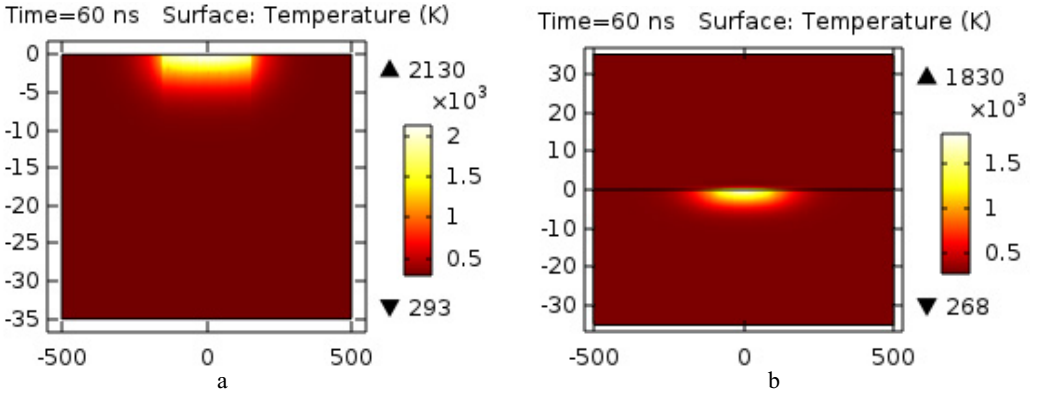

Figure 10: 2D Temperature profile obtained for 532 nm laser wavelength after 60 ns a) in air b) underwater

It was observed experimentally using 20 J/cm^2 fluence for 3, 4 and 5 pulses, the depth achieved is 3.6, 4.3 and 5.2, respectively. From this data, it is inferred that for one pulse the depth is ~ 1 μm. The depth achieved for 532 nm from the present model at 3000 K is thus validated with the experimental data. Figure 9 shows the temperature profile estimated for the 3 wavelengths for Cu sample. In the developed model, as we have not incorporated the effect of plasma and the change in material properties with temperature, both 355 nm and 532 nm laser follow the same trend, but since the reflectivity of 1064 nm for same fluence is high the temperature reached at the surface is less than 355 nm and 532 nm. Same is the case with recession rate estimated and shown in Figure 10. This is also proved experimentally that 1064 nm gives lesser depth compared to shorter wavelengths. This model can further be developed by incorporating the effect of temperature on the material properties of the work piece in order to correctly predict the laser material interaction. Figures 9(a) and b show the temperature profiles of copper thin film in air and underwater ambience conditions. Water layer is shown as 0 to -10 μm as seen in the X-axis in Figure 9(b) it is observed that heat conducts from the workpiece to the water medium. Figure 10(a), (b) shows the 2D temperature profile of the copper thin film after 60 ns in air and underwater respectively, underwater sample cools faster than the air sample as seen from the temperature scale.

5 Conclusions

Comparison of different laser wavelengths, namely 355 nm, 532 nm and 1064 nm on scribing of the micro-channel in Cu / Al films was carried out. For aluminum in air medium, the channel depth obtained is high for 355 nm wavelength, whereas for copper coated on a polyimide substrate, 532 nm wavelengths produced higher depth. As the input energy increased, the width of channel also increased initially but with the input energy greater than 6 mJ, the change in width was limited to few microns. As water level decreased, ablation rate became high and depth of channel increased. It was observed that shorter wavelength ablates more effectively compared to longer wavelength in water medium in case of Al, whereas for Cu, longer wavelength ablated more material in water medium compared to air. Melt pool was observed in dry (air) ablation but it was not seen in underwater ablation. No re-deposition at the edges is observed when micro scribing is done in de-ionized water medium. Recession rate during the laser scribing was estimated based on the theoretical model by combining the ablated plume temperature measured using the laser induced breakdown spectroscopy technique.

References

Aurich J C, Dornfeld, D Arrazola, P J Franke, V Leitz, L and Min S. Burrs—Analysis, control and removal. *CIRP Annals-Manufacturing Technology* 2009; 58(2): 519-542.

Bogaerts A, Chen Z, Gijbels R and Vertes A. Laser ablation for analytical sampling: what can we learn from modeling?. *Spectrochimica Acta Part B: Atomic Spectroscopy* 2003; 58(11): 1867-1893.

Chien W T and Hou S C. Investigating the recast layer formed during the laser trepan drilling of Inconel 718 using the Taguchi method. *The International Journal of Advanced Manufacturing Technology* 2007; 33(3-4): 308-316.

Choo K L, Ogawa Y, Kanbargi G, Otra V, Raff L M and Komanduri R. Micromachining of silicon by short-pulse laser ablation in air and underwater. *Materials Science and Engineering A* 2004; 372(1): 145-162.

Compaan A D, Matulionis I, Miller M and Jayamaha U N. Optimization of laser scribing for thin-film photovoltaics. *Photovoltaic Specialists Conference*,1996, Conference Record of the Twenty Fifth IEEE, 1996 ,pp. 769-772.

Descoeudres A, Hollenstein C, Demellayer R. and Wälder G. Optical emission spectroscopy of electrical discharge machining plasma. *Journal of materials processing technology* 2004; 149(1): 184-190.

Fabbro R, Fournier J, Ballard P, Devaux D and Virmont J. Physical study of laser-produced plasma in confined geometry. *Journals of Applied Physics* 1990; 68: 775-784

Jackson M. J and O'Neill W. Laser micro-drilling of tool steel using Nd: YAG lasers. *Journal of Materials Processing Technology* 2003; 142(2): 517-525.

Kruusing A. Underwater and water-assisted laser processing: Part 2—Etching, cutting and rarely used methods. *Optics and Lasers in Engineering* 2004; 41(2): 329-352.

Krstulović N, Shanno, S, Stefanuik R and Fanara C. Underwater-laser drilling of aluminum. *The International Journal of Advanced Manufacturing Technology* 2013; 69(5-8): 1765-1773.

Lee J M, Curran C and Watkins K G. Laser removal of copper particles from silicon wafers using UV, visible and IR radiation. *Applied Physics A* 2001; 73(2): 219-224.

Lu J, Xu Q, Chen X, Shen Z H, Ni X W, Zhang S Y and Gao C M. Mechanisms of laser drilling of metal plates underwater. *Journal of applied physics* 2004; 95(8): 3890-3894.

Palik E D. (Ed.). *Handbook of Optical Constants of Solids*, Five-Volume Set: Handbook of Thermo-Optic Coefficients of Optical Materials with Applications 1997. Academic Press.

Peyre P and Fabbro R. Laser shock processing: a review of the physics and applications. *Optical and Quantum Electronics* 1995; 27(12): 1213-1229.

Stafe M, Negutu C and Ducariu A N. Pulsed laser ablated craters on aluminum in gaseous and aqueous environments. *Romanian Reports in Physics* 2012; 64(1): 155-162.

Tunna L, Kearns A, O'neill W and Sutcliffe C J. Micromachining of copper using Nd: YAG laser radiation at 1064, 532, and 355 nm wavelengths. *Optics & Laser Technology* 2001; 33(3):135-143.